Oceanological and Hydrobiological Studies

International Journal of Oceanography and Hydrobiology

Volume 45, Issue 2, June 2016
pages (230-238)

ISSN 1730-413X
eISSN 1897-3191

Determination of the oil spill removal area by oil particle tracking in a harbor

by

Shu-Yi Yang, Xue-Yi You*

DOI: **10.1515/ohs-2016-0021**
Category: **Original research paper**
Received: **May 25, 2015**
Accepted: **August 19, 2015**

Tianjin Engineering Center of Urban River Eco-purification Technology, School of Environmental Science and Engineering, Tianjin University, Tianjin 300072, China

Abstract

The removal of oil spill pollution is an important issue of water environment protection. A hydrodynamic model for the determination of oil spill removal area is proposed based on the Euler-Lagrangian particle tracking method. After the results of flow field simulation are validated by the measured data, the trajectory of oil particles is calculated. The optimal location of oil spill removal area is obtained by comparing the oil removal rate of different removal areas. The current method presents a useful way of locating the optimal oil spill removal area to clean the surface waters.

Key words: oil spill, oil particle tracking, removal area, surface water, EFDC model

* Corresponding author: *xyyou@tju.edu.cn*

DE GRUYTER

The *Oceanological and Hydrobiological Studies* is online at oandhs.ocean.ug.edu.pl

Introduction

The ocean is a treasure of natural resources as well as an important driving force for economic development of coastal states. In recent years, the global oil demand is growing along with the rapid growth of sea freight volume. With the increasing number of oil tankers, oil spill accidents cause an increase in the risk to the aquatic environment of a port (Abdul et al. 2012; Lan et al. 2014).

An oil spill not only causes huge economic losses, but also a great damage to the ecological environment of marine waters. The oil spill movement is complex and variable, so that the development of an effective clean-up method becomes an urgent and difficult issue in the protection of the marine environment.

Along with the improvement in numerical methods and computers, numerical modeling is becoming a useful tool to predict the fate of an oil spill and to assist in the fight and contingency planning for environmental catastrophes. Since the early 1960s, the United States and many European countries began to take the lead in marine oil spill studies and developed many oil spill dynamic models (Alberto et al. 2014; Jason et al. 2014). Oil spill processes are described mathematically with varying degrees of complexity. There are many examples of oil spill modeling, including the Oil Drift 3 Dimensional Model OD3D (Brostrom et al. 2011; Wettre et al. 2011), the Meteo France Oil Spill Forecast System MOTHY (Daniel et al. 2004), the Japan Meteorological Agency Oil Spill Prediction OLIMAP (Spaulding et al. 1992), the General NOAA Operational Modeling Environment GONME (Cheng et al. 2011; Xu et al. 2013), the Environmental Fluid Dynamic Code Model EFDC (Deng et al. 2011).

The majority of current oil spill models are particle-tracking models. In the case of an oil spill, the oil film is in the motion under the impact of wind forces and surface flow. The Lagrangian particle tracking model describes the migration path of an oil spill and has been widely applied in the prediction of many marine oil spill accidents (Abascal et al. 2010; Martinho et al. 2013; Romero et al. 2013).

Oil spill removal by cleaning up facilities with fixed position is a highly efficient, passive way of oil spill collection, which requires only little manual operation and small financial resources. This paper presents a method for determining the optimal oil removal area based on the hydrodynamic EFDC model, where trajectories of oil spill particles are drawn with the deterministic Lagrangian method to simulate the translation process and the uncertainty random walk method to simulate the disturbance process. By tracing the moving path of oil spill particles, the efficiency of oil spill cleaning up of different removal areas is determined, and the optimal removal area is found for an engineering layout.

Materials and methods

Hydrodynamic model

A hydrodynamic model is the foundation of trajectory prediction of oil spill particle. The widely used EFDC model is used to provide the dynamic flow field and oil particle movement. This model is developed by John Hamrick (Hamrick 1992, 1995; Hamrick & Wu 1997). It is one of the most respected models and has been widely used by universities, the government and environmental consulting in a wide variety of fields (Shen and Haas 2004; Xu et al. 2008; Gong et al. 2009; Wang et al. 2010; Gong et al. 2012; Zhao et al. 2013). In this model, turbulence is included in the second moment turbulence closure model developed by Mellor and Yamada (1982) and modified by Galperin et al. (1988). Turbulent viscosity and diffusivity is related to the turbulent intensity, the turbulence mixing length and the Richardson number. The controlling equations of the EFDC model can be found in Hamrick (1992).

Particle tracking

The macroscopic motion of oil spill particles is simulated by the particle tracking model of the Lagrange method. The particle diffusion process caused by turbulence is random. It is simulated by the random walk method, namely the motion of particles in a turbulent flow field is similar to the random movement of molecules.

The particle tracking model with the random walk of particles is written as follows:

$$dx = dx_{drift} + dx_{ran} = \left(u + \frac{\partial D_H}{\partial x}\right)dt + \sqrt{2D_H dt}\,(2p-1) \quad (1)$$

$$dy = dy_{drift} + dy_{ran} = \left(v + \frac{\partial D_H}{\partial y}\right)dt + \sqrt{2D_H dt}\,(2p-1) \quad (2)$$

$$dz = dz_{drift} + dz_{ran} = \left(w + \frac{\partial D_z}{\partial z}\right)dt + \sqrt{2D_z dt}\,(2p-1) \quad (3)$$

where, t is time, (x,y,z) is Lagrangian coordinates of a particle, $\vec{V}=(u,v,w)$ is flow velocity, u , v and w stand for the velocity in the direction of x, y, z, respectively. D_H and D_z are the horizontal and vertical diffusion coefficients, respectively, dt is time step and p with the mean value of 0.5 is a random number from a uniformly distributed random variable generator. The above equations are solved by the fourth-order Runge-Kutta method.

Model descriptions

Flow domain

Tianjin Nangang is selected as the study area. It is an important part of the Tianjin port. It is located in the east of Bohai Bay (Fig. 1). The development and construction of the Tianjin Nangang industrial zone is an important strategy of the Tianjin city. The eastern harbor reclamation project has been established and the removal of oil spills leaked by ships is a key issue in preserving the good quality of water and in the development of tourism. The study area is surrounded by the north and east breakwaters of Nangang. The wave action is very weak in sheltered waters and the impact of surface waves is not taken into account.

Figure 1

The Port of Tianjin in the Bohai Sea (satellite images from bing maps)

Grid setup

A multi-nested grid model was used to perform an accurate analysis. It consists of the Tianjin port model and the Nangang model presented in Figs 2 and 3. In the computational domain, the seabed is almost flat and the depth of water from the shore gradually increases to about 20 m at the open-sea boundary. The ports and waterways are about 15 m deep.

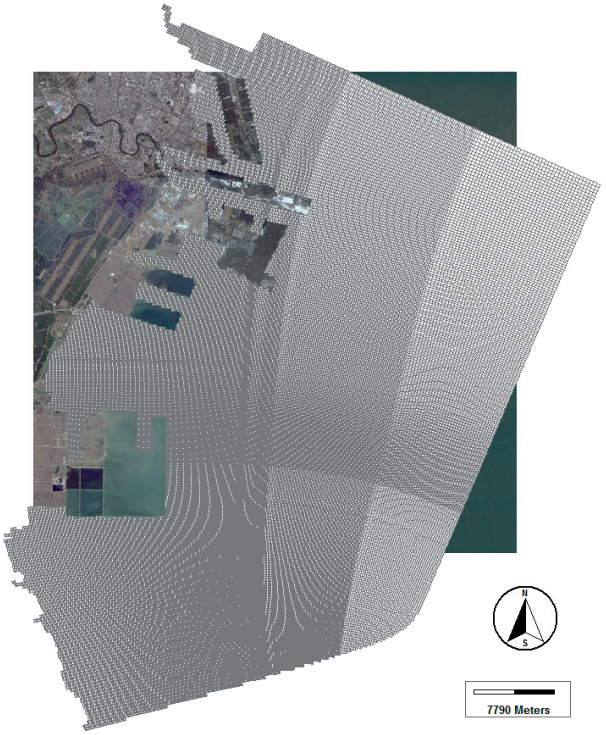

Figure 2

The grid of the Tianjin port model (satellite image from bing maps)

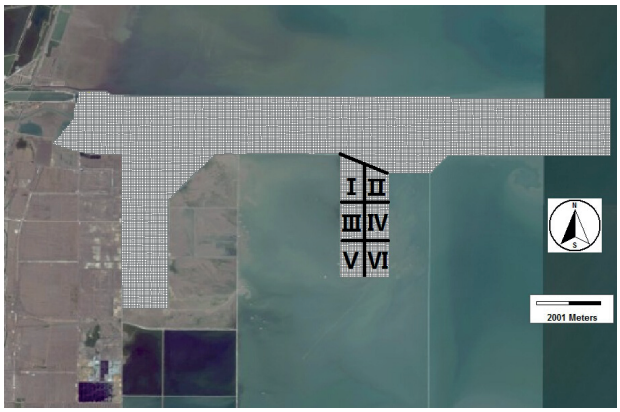

Figure 3

The grid of Nangangmodel with the six simulation oil spill regions in the eastern harbor of Tianjin Nangang (satellite image from bing maps)

The Tianjin port model has 49221 horizontal grids. The sufficient grid resolution is provided to effectively present the coastline as well as sufficient details of a specific area to support the detailed modeling. Curvilinear grids are used in the domain, and the spatial resolution ranges from 50 m in the nearshore zone to 1000 m in the far-shore zone. In order to ensure the accuracy of the surface wind flow and the bottom friction stress, three layers are selected in the vertical direction.

Model details

The initial conditions of the Tianjin port model are water level and flow velocity. As the water level and flow velocity follow rapidly towards the external dynamic response, the cold start mode sets the initial water level as the mean water level and the initial velocity to zero. The water elevation at the open boundary is given by the nearest neighbor interpolation. The area adjacent to the sea is mostly the muddy coast and the seabed is smooth. After several debugging processes, the roughness is selected as 0.022 for the best fit of data. The horizontal momentum diffusion coefficient is calculated according to Smagorinsky's formula and the mixed constant level is 0.1. The horizontal eddy viscosity coefficient is the same with the turbulent diffusivity of momentum. The model time step is 2 s based on the CFL condition, which is determined by the grid dimension and the velocity in the adjacent sea area. For a model run of 100 days, the computer runtime is about 4.5 days on a Dell T5500 workstation with 12 processors.

The nested Nangang model has 17522 horizontal grids with the size of 50 m. The same parameter settings, such as the vertical roughness, bottom roughness and the time step, are used for the Tianjin port model. The horizontal momentum diffusion coefficient is also calculated by the Smagorinsky formula. The water level is provided by the results of the Tianjin port model. The initial simulation starts with calm water conditions without a wind field. The time step of the nested model is also 2 s. For a run of 100 days of the nested model with tracing three thousand oil particles, the computer runtime is about 5 days on a Dell T5500 workstation with 12 processors.

Model validations

The water level and the magnitude and direction of velocity are compared with the field monitoring data. Stations monitoring the water level and flow velocity are shown in Fig. 1. Figs 4-6 show that the numerical results are consistent with the measured data during low and high tide periods. Furthermore, the numerical results are also in line with the measured data during low and high tide periods at the two other velocity monitoring stations, which are not shown in this paper for the sake of brevity. It is evidenced that our numerical model can well simulate the flow field.

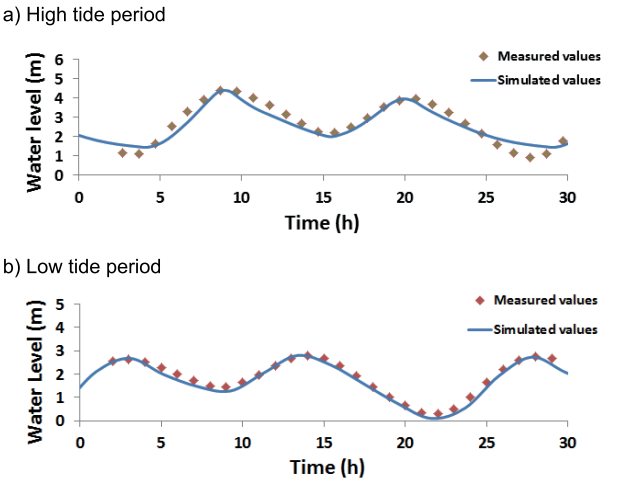

Figure 4

Model validation of the water level at the water level monitoring station

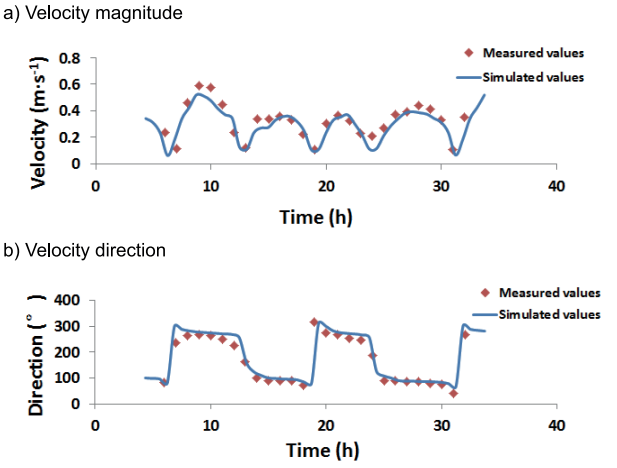

Figure 5

Model validation of the velocity magnitude and direction at monitor station 2 during the high tide period

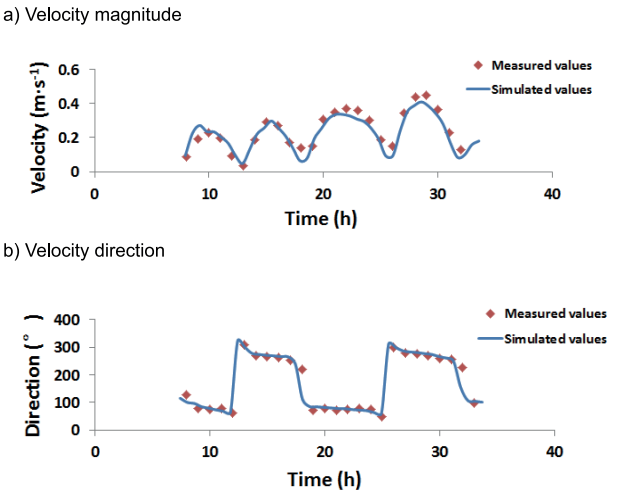

Figure 6

Model validation of the velocity magnitude and direction at monitor station 2 during the low tide period

Results and discussion

Motion of tracer particles in different regions

In order to determine the optimal removal area of an oil spill, the particle tracking model is introduce to simulate the trajectory of oil particles based on the flow field of the Nangang model. The possible oil spill area is divided into six regions based on the characteristics of a harbor shown in Fig. 3. Regions I, III and V correspond to a coal or ore berth on the west side of the harbor. Regions II, IV and VI correspond to an LNG reservoir, a petrochemical berth and a universal berth on the east side of the harbor. The drift process of an oil spill is described by a movement of oil particles. Particles are put in the center of each grid of a region to represent the movement of an oil spill within a given region. At each time step, the new position of oil particles is computed by considering the transport induced by currents, wind and turbulent dispersion.

Fig. 7 shows the trajectory pattern of oil particles in different regions. Particles from regions I, II and III have a wide sweeping area. In addition to moving in the offshore direction, some of them can even move toward the west basin. Particles from regions IV, V and VI are exchanged mainly offshore. A small part of particles from region III and a few particles from regions I, II and IV migrate to the bottom of the basin. Particles from regions I, II, III and IV migrate from the harbor in a short time while those from regions V and VI take a long time. This is due

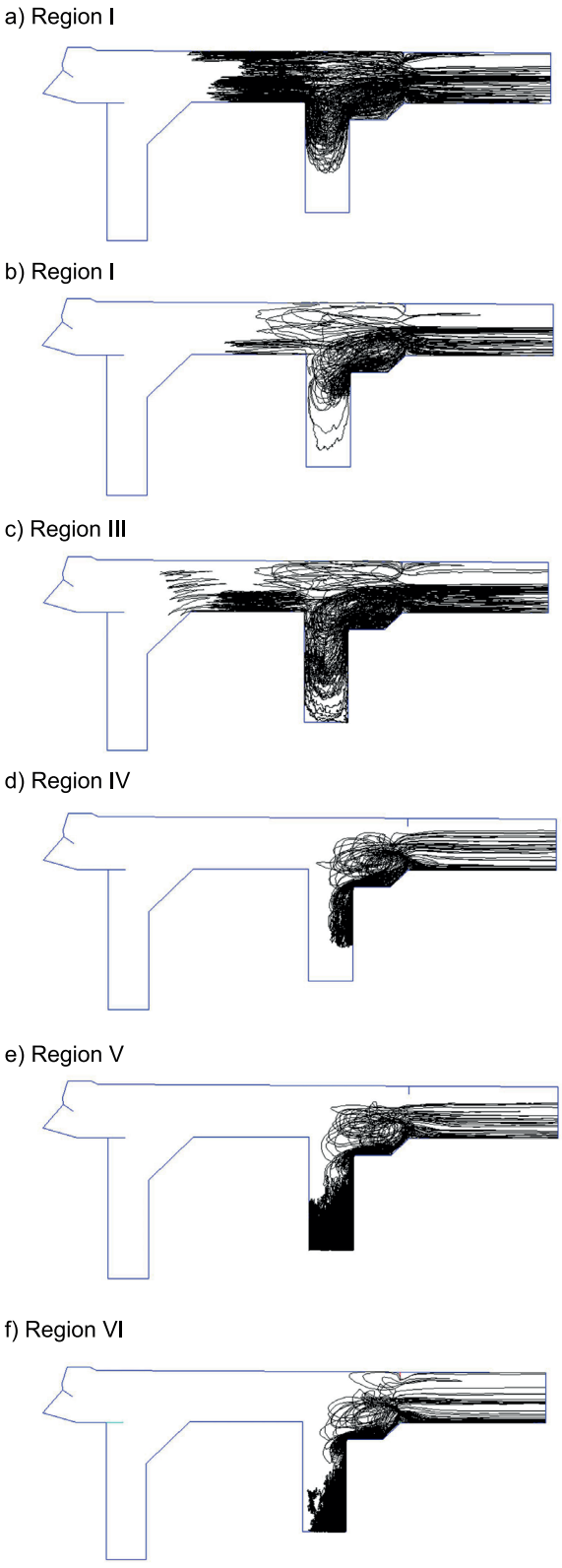

Figure 7

Trajectory of oil particles from different regions (no wind)

to the fact that regions V and VI are characterized by low water exchange capacity.

It has been found that many of the particles pass through the south breakwater before they move offshore. Thus, it makes sense that the oil removal area is located in the vicinity. In this approach, other possible areas are also selected to study the effect of oil removal in different oil spill areas.

By considering the trajectory of oil particles, the sweeping area of an oil spill is determined for a given removal area. The position of different removal areas is shown in Fig. 8. By comparing the oil removal rate of different areas, the area with the highest efficiency in oil removal is selected.

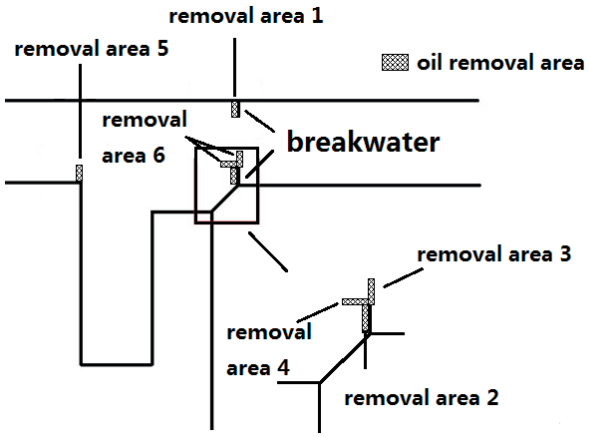

Figure 8

Position of different oil removal areas

Removal rate of different removal areas

According to the trajectory of particles, six areas are selected for the potential location of the oil removal area. In this method, particles moving through the removal areas are assumed to be removed completely from the computational domain and the number of removed particles is counted by a Matlab program which can acquire data on the movement of particles from the particles tracking models in EFDC. The ratio of the removed particles to the total particles is referred to in this paper as the removal rate.

Each of oil removal areas 1, 2, 3 and 5 has a length of 300 m and a width of 50 m. Oil removal area no. 4 has a length of 50 m and a width of 300 m. Oil removal area no. 5 is a combination of oil removal areas no. 3 and 4.

Of the above 6 oil spill removal areas, particles from region III have the largest sweep range and they are used as an example to show the oil removal result of different oil removal areas. Fig. 9 shows the trajectory of oil particles from region III after 100 days of the oil removal operation for different oil removal areas. The oil removal rate of oil removal areas 2, 3, 4 and 6 significantly reduces the oil particles from regions III. The oil removal rate of removal area no. 6 has the largest oil removal rate.

Removal area no. 5 is located in the northwest of the harbor. If this area is selected as an oil removal area, only oil particles from regions I, II and III moving to the west are removed and those from regions IV, V and VI are removed in small numbers. Therefore, the oil removal rate of removal area no. 5 is low.

Oil removal area no. 1 near the north breakwater is the least efficient oil removal position. It can only remove a few oil particles from regions I, II and III and it cannot remove the oil spill from regions IV, V and VI.

Season effects

The study area is located in the monsoon climate zone. The wind shows different characteristics in different seasons. The wind has a strong effect on the movement of an oil spill. Table 1 shows the direction, speed and probability of prevailing wind in each season. It has been found that the probability of prevailing wind in each season is about 15%. This means that the prevailing wind occurs in about 60% of the days in a year. Therefore, the seasonal prevailing wind is considered as the simulation wind of the season.

Table 1

Speed, direction and probability of prevailing wind based on the local climate data

Season	Wind Direction	Wind Speed ($m\ s^{-1}$)	Probability (%)
Spring	SW	5.0	15
Summer	SWS	4.1	12
Autumn	S	4.5	15
Winter	N	4.5	13

The oil removal rate is defined as the ratio of the number of removed oil particles to the number of initial total oil spill particles in the harbor. Table 2 shows the oil removal rate at different removal areas after 100 days of the oil removal operation. It has been found that oil removal areas no. 1 and 5 always

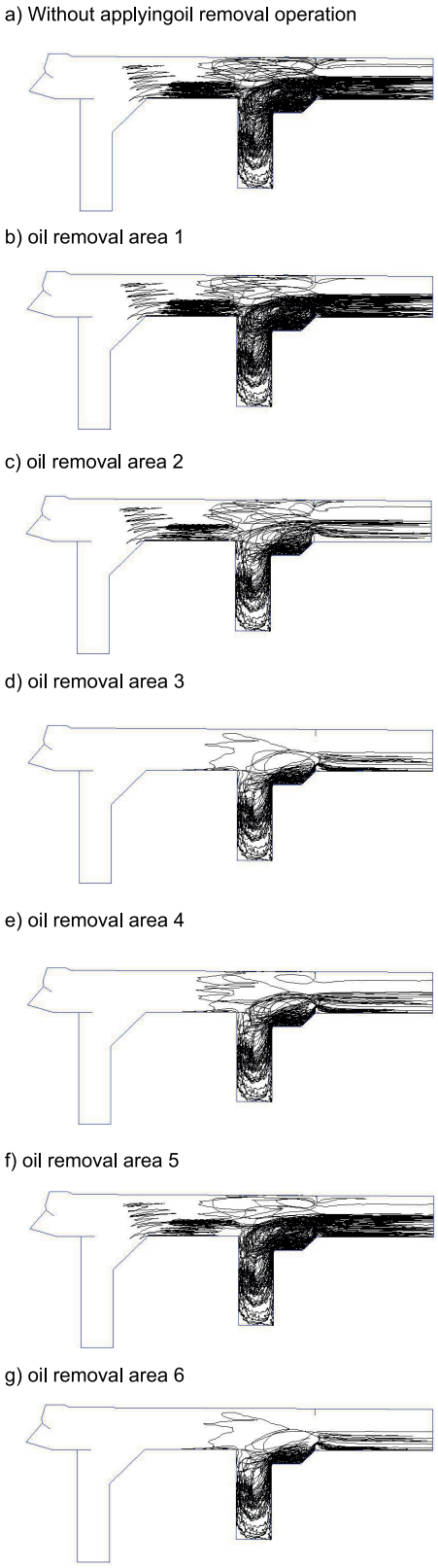

Figure 9

Trajectory of oil particles from region III after 100 days of the oil removal operation in different oil removal areas

Table 2

Removal rate of oil spill in the harbor after 100 days of the oil removal operation in different removal areas (%)

Removal area	No wind	Spring	Summer	Autumn	Winter	Annual Average
1	7.5	1.3	3.1	7.5	9.6	5.4
2	62.3	65.8	70.6	44.3	20.6	50.3
3	74.6	85.5	89.9	74.1	64.9	78.6
4	66.7	80.7	84.2	74.1	72.4	77.9
5	18.4	11.4	15.4	17.1	22.8	16.7
6	77.6	87.7	92.5	79.8	79.4	84.5

show poor performance. Removal area no. 2 is easily affected by wind. Its removal rate increases in spring and summer; however, it significantly decreases in autumn and winter, especially in winter. Compared to no-wind conditions, removal areas no. 3, 4 and 6 with a seasonal wind show high removal rates. The removal ratio of removal areas 3, 4 and 6 is about 80% throughout the year. Considering the fact that removal area no. 6 overlaps with removal areas no. 3 and 4 and removal area 3 is on the cross-section of the harbor gate, removal area 4 is selected as an optimal area for the oil spill removal in the harbor.

Conclusions

The location method for the oil spill removal area is proposed based on the oil particle tracking method by applying the EFDC software. In this approach, a two-level nested grid model is developed to predict the movement of an oil spill. After the flow field verification, the oil spill in a harbor is tracked by oil particles allowing for the local meteorological wind conditions. The optimal removal area is determined for the oil spill removal in a harbor. The main conclusions are as follows:

(1) The oil removal range of different removal areas is high. In the present study, it ranges from 5% to 85% after 100 days of the oil removal operation. The selection of the optimal oil removal area is very important for improving the oil removal efficiency;

(2) The oil removal efficiency of the oil removal area strongly depends on the relative position of the oil removal area and the oil spill area. The optimal oil removal area can be selected by the

oil particles tracking method.

(3) The removal rate of different removal areas is strongly affected by local meteorological wind conditions. The direction, speed and probability of prevailing wind in each season should be considered when the optimal oil removal area is determined by the present method.

(4) The proposed method can also be used to determine the optimal clean-up area for the removal of floating garbage in rivers and lakes.

Acknowledgement

This work was supported by the key projects in the control and management of national polluted water bodies (2014ZX07203-009) and the science and technology project of Nangang Port Co. Ltd. of the Tianjin Port Group.

References

Abascal, A.J., Castanedo, S., Medina, R. & Liste, M. (2010). Analysis of the reliability of a statistical oil spill response model. *Marine Pollution Bulletin* 60: 2099-2110. DOI: 10.1016/j.marpolbul.2010.07.008.

Abdul, A., Abdulrauf, R.A. & M. Enamul, H. (2012). A sustainable approach to controlling oil spills. *Journal of Environmental Management* 113: 213-227. DOI: 10.1016/j.jenvman.2012.07.034.

Alberto, A., Anabela, O., Andre & B.F (2014). A Cross-scale Numerical Modeling System for Management Support of Oil Spill Accidents. *Marine Pollution Bulletin* 80: 132-147. DOI: 10.1016/j.marpolbul.2014.01.028.

Cheng, Y.C., Li, X.F., Xu, Q., Oscar, G.P. & Andersen, B.O. (2011). SAR observation and model tracking of an oil spill event in coastal waters. *Marine Pollution Bulletin* 62: 350-363. DOI: 10.1016/j.marpolbul.2010.10.005.

Daniel, P., Josse, P. & Dandin, P. (2005). Further improvement of drift forecast at sea based on operational oceanography systems. *In: Coastal Engineering VII: Modelling, Measurements, Engineering and Management of Seas and Coastal Regions*. WIT Press, pp. 13-22.

Deng, J., Huang, L., Zhao, Q., Liu, J. & Wang, X. (2011). Study on prediction model of oil spill in Three Gorges Reservoir Area based on a two-dimensional hydrodynamic coupling simulation. *Journal of wuhan university of technology* 35: 793-797.

Gong, W., Shen, J. & Hong, B. (2009). The influence of wind on the water age in the tidal Rappahannock River. *Marine Environmental Research* 68: 203-216. DOI: doi:10.1016/j.marenvres.2009.06.008.

Gong, W., Wang, Y. & Jia, J. (2012). The effect of interacting downstream branches on saltwater intrusion in the Modaomen Estuary, China. *Journal of Asian Earth Sciences* 45: 223-238. DOI: 10.1016/j.jseaes.2011.11.001.

Hamrick, J.M. (1992). *A three-dimensional environmental fluid dynamics computer code: theoretical and computational aspects*. Special Report 317. The college of William and Mary, Virginia Institute of Marine Science, Williamsburg Virgina, 63pp.

Hamrick, J.M. & Wu, T.S. (1997). *Computational design and optimization of the EFDC/HEM3D surface water hydrodynamic and eutrophication models*. In G. Delic & M.F. Wheeler (Eds.), Next Generation Environmental Models and Computational Methods. Society for Industrial and Applied Mathematics, Pennsylvania, pp. 143-161.

Jason, K.J., Travis, A.S. & Sherwin, L. (2014). Simulating Surface Oil Transport During the Deepwater Horizon Oil Spill: Experiments with the BioCast System. *Ocean Modelling* 75: 84-99. DOI: 10.1016/j.ocemod.2014.01.004.

Lan, D., Bao, C. & Ma, M. (2014). Technique to Marine Oil Spill Risk Zonation and its Application. *Marine Environment Science* 33: 287-292.

Marta-Almeida, M., Ruiz-Villarreal, M., Pereira, J., Otero, P., Cirano, M. et al. (2013). Efficient tools for marine operational forecast and oil spill tracking. *Marine Pollution Bulletin* 71: 2099-2110. DOI: 10.1016/j.marpolbul.2013.03.022.

Romero, A.F., Abessa, D.M.S., Fontes, R.F.C. & Silva, G.H. (2013). Integrated assessment for establishing an oil environmental vulnerability map: Case study for the Santos Basin region, Brazil. *Marine Pollution Bulletin* 74: 156-164. DOI: 10.1016/j.marpolbul.2013.07.012.

Shen, J. & Haas, L. (2004). Calculating age and residence time in the tidal York River using three-dimensional model experiments. *Estuarine, Coastal and Shelf Science* 61 (3): 449-461. DOI: doi:10.1016/j.ecss.2004.06.010.

Spaulding, M.L. (1988). A state-of-the-art review of oil spill trajectory and fate modelling. *Oil Chem. Pollut.* 4: 39-55. DOI: doi:10.1016/S0269-8579(88)80009-1.

Wang, Y., Shen, J. & He, Q. (2010). A modeling study of the variation of the transport timescale and change of estuarine circulation due to human impact in the Changjiang Estuary, China. *Journal of Marine Systems* 82 (3): 154-170.

Wettre, C., Johansen, O. & Skognes, K. (2011). *Development of a 3-Dimensional Oil Drift Model at DNMI*. Tech. Rep. 50, Norwegian Meteorological Institute, Oslo, Norway.

Xu, H., Lin, J., Shen, J. & Wang, D. (2008). Wind impact on pollutant transport in a shallow estuary. *Acta Oceanologica*

Sinica 27 (3): 147-160.

Xu, Q., Li, X.F., Wei, Y.L., Tang, Z.Y., Cheng, Y.C. et al. (2013). Satellite observations and modeling of oil spill trajectories in the Bohai Sea. *Marine Pollution Bulletin* 71, 107-116. DOI: 10.1016/j.marpolbul.2013.03.028.

Zhao, L., Li, Y., Zou, R., He, B., Zhu, X. et al. (2013). A three-dimensional water quality modeling approach for exploring the eutrophication responses to load reduction scenarios in Lake Yilong (China). *Environmental Pollution* 177: 13-21. DOI: 10.1016/j.envpol.2013.01.047.